Expanded View Figures

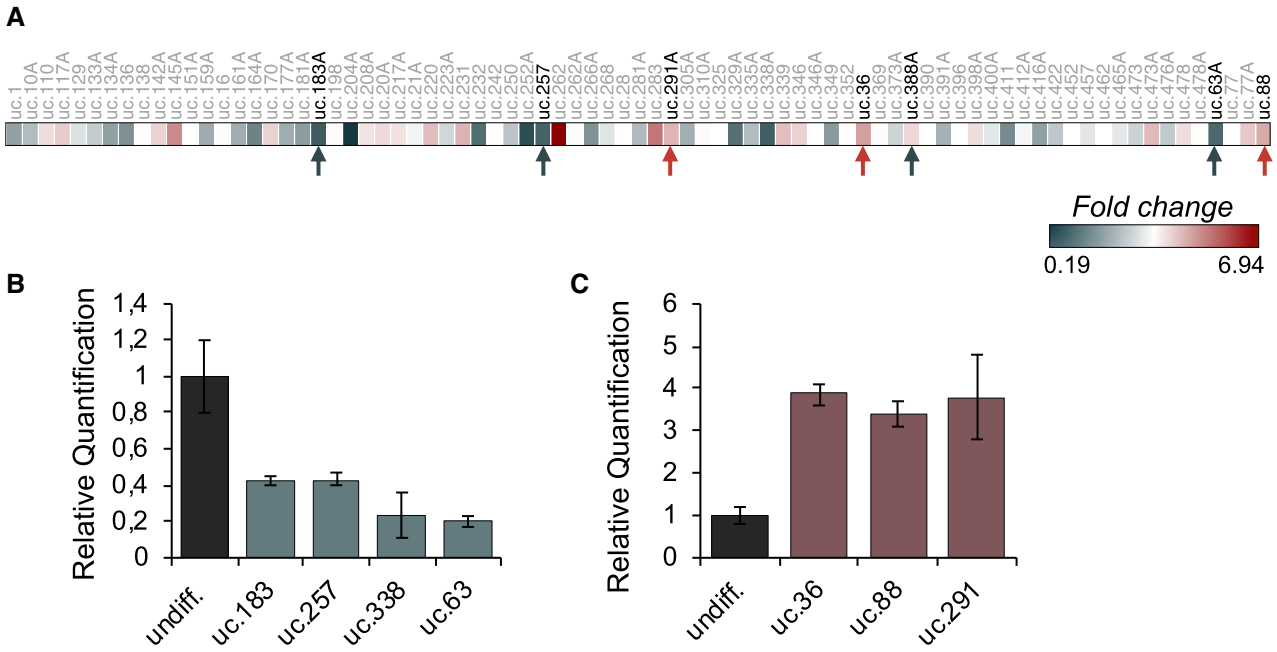

Figure EV1. UC RNA is modulated during keratinocyte differentiation.

A Heatmap showing microarray data results. Data are expressed as fold change.

B Validation by RT–qPCR of down-regulated UCs showed in (A).

C Validation by RT–qPCR of up-regulated UCs showed in (A). In (B) and (C), the quantification is relative to the same UC expression in undifferentiated HEKn (undiff., dark grey bars); data shown represent the mean ± standard error (RT–qPCR has been done in triplicate); n = 1 (technical).

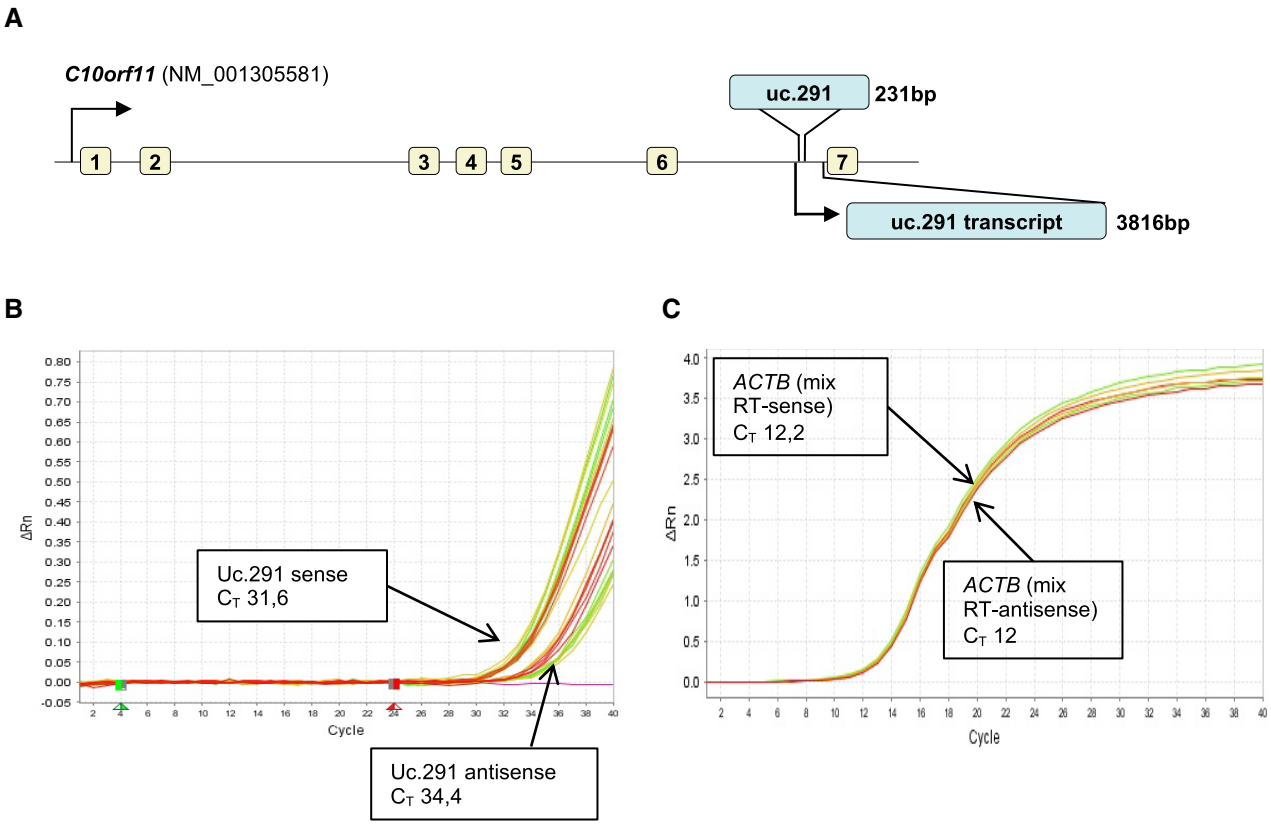

Figure EV2. Characterization of uc.291 transcript by strand-specific RT–qPCR.

A Uc.291 (3,816 bp) genomic location on chromosome 10 in the sixth intron of the *C10orf11* gene.

B Uc.291 strand-specific RT–qPCR; representative amplification plots (#2 of Fig 1G) of strand-specific RT–qPCR; qPCR curves relative to the sense and the antisense transcripts are shown.

C *ACTB* mRNA strand-specific RT–qPCR was used as control.

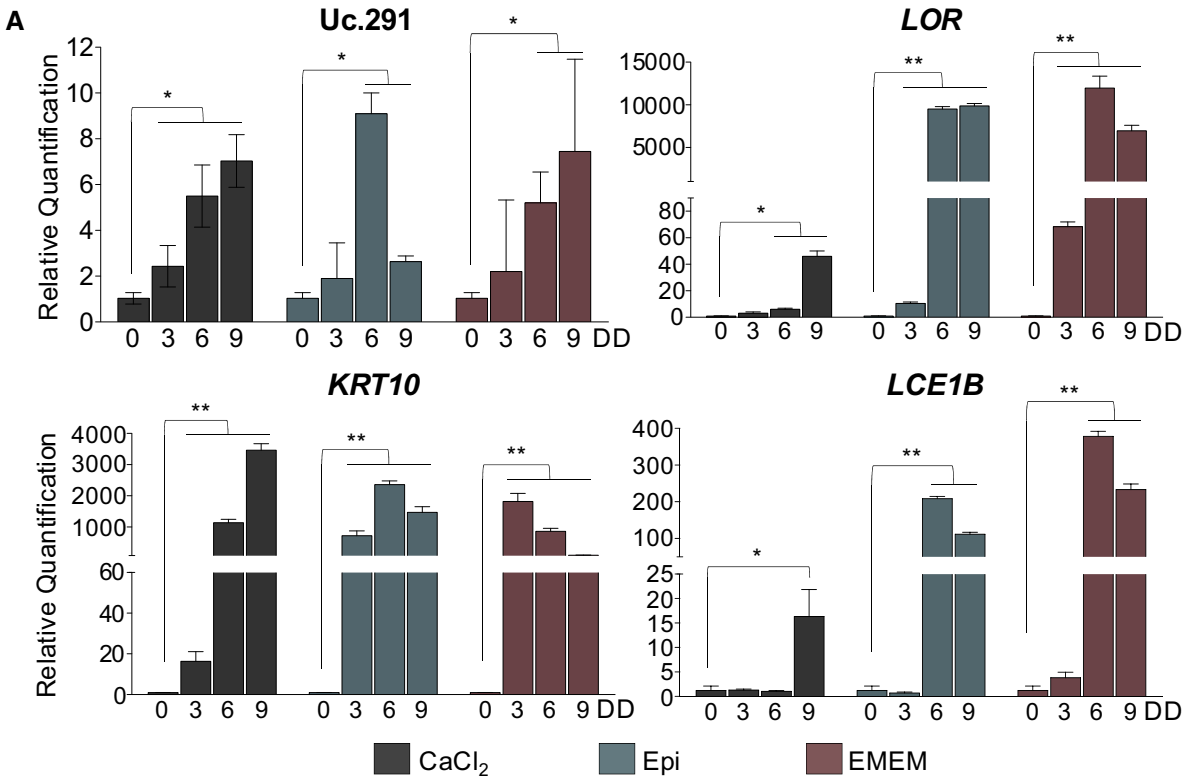

Figure EV3. uc.291 is up-regulated during keratinocyte differentiation, regardless of the differentiation methodology.

A RT–qPCR showing uc.291 expression in HEKn grown in calcium-induced differentiation ($CaCl_2$) or confluence-induced differentiation (in Epi and EMEM). $CaCl_2$ = calcium chloride; Epi = EpiLife; EMEM = Eagle's minimum essential medium. *LOR*, *KRT10* and *LCE1B* were used as differentiation markers. DD = days of differentiation; the quantification is relative to the same expression in undifferentiated HEKn (0 DD); data shown represent the mean ± standard deviation; $n = 3$ (technical); $^{*}P < 0.05$, $^{**}P < 0.01$, Student's *t*-test.

B Box plot showing quantification of Ki67-positive nuclei on total nuclei. In parallel with the increase of p63 expression (Fig 2), depletion of uc.291 affects the proliferation rate of basal keratinocytes. Each central line represents the *median*; each box represents *Q1* (quartile 1, below the median) and *Q3* (quartile 3, above the median); the whiskers represent *minimum* (Q1 − 1.5*IQR) and *maximum* (Q3 + 1.5*IQR). IQR = interquartile range; 15, 14 and 15 images were analysed for SCR, si-uc.291 (1) and si-uc.291 (2), respectively; $^{*}P < 0.05$; $^{**}P < 0.01$, Student's *t*-test.

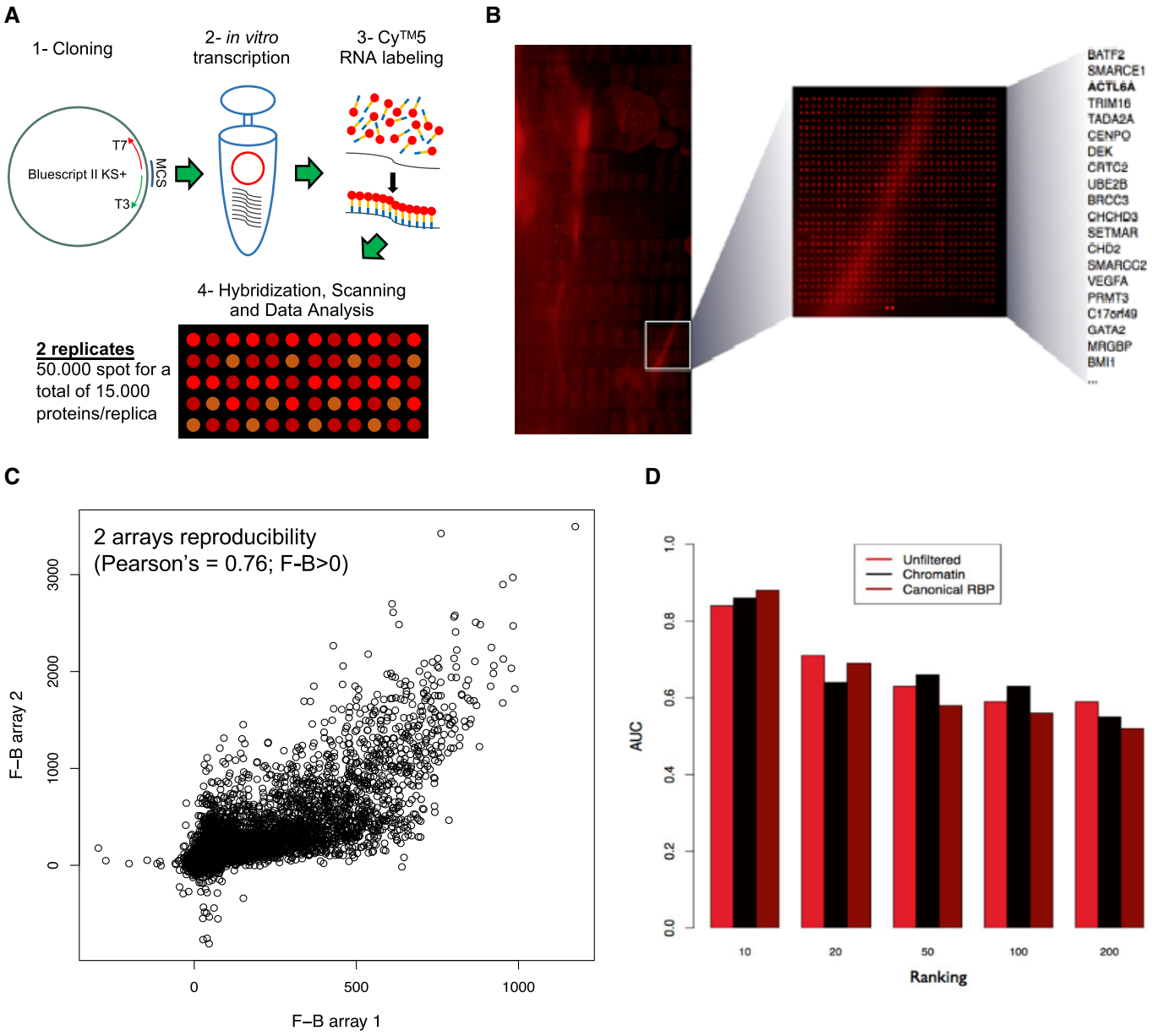

Figure EV4. Uc.291 protein microarray.

A Schematic depicting high-throughput analysis performed to identify uc.291 protein interactome.

B Protein array analysis showing the top 20 chromatin-related candidates; see also Appendix Table S2.

C Reproducibility between the two human recombinant protein arrays spotted with 50,000 different proteins. (Pearson's correlation = 0.76; F-B > 0).

D Area under ROC curve (AUC) to assess Global Score [34] ability to separate proteins interacting with uc.291 from those that are non-interacting. The F-B score was employed to select different groups of high-affinity (top ranked) and low-affinity (bottom ranked) interactions reported in the array: (1) RBP, (2) chromatin-related and (3) unfiltered (i.e. without selecting by category). In all cases, Global Score performances increase from poor signal (top/bottom 200) to strong signal (top/bottom 10) interactions, showing AUCs that raise from 0.60 to 0.80.

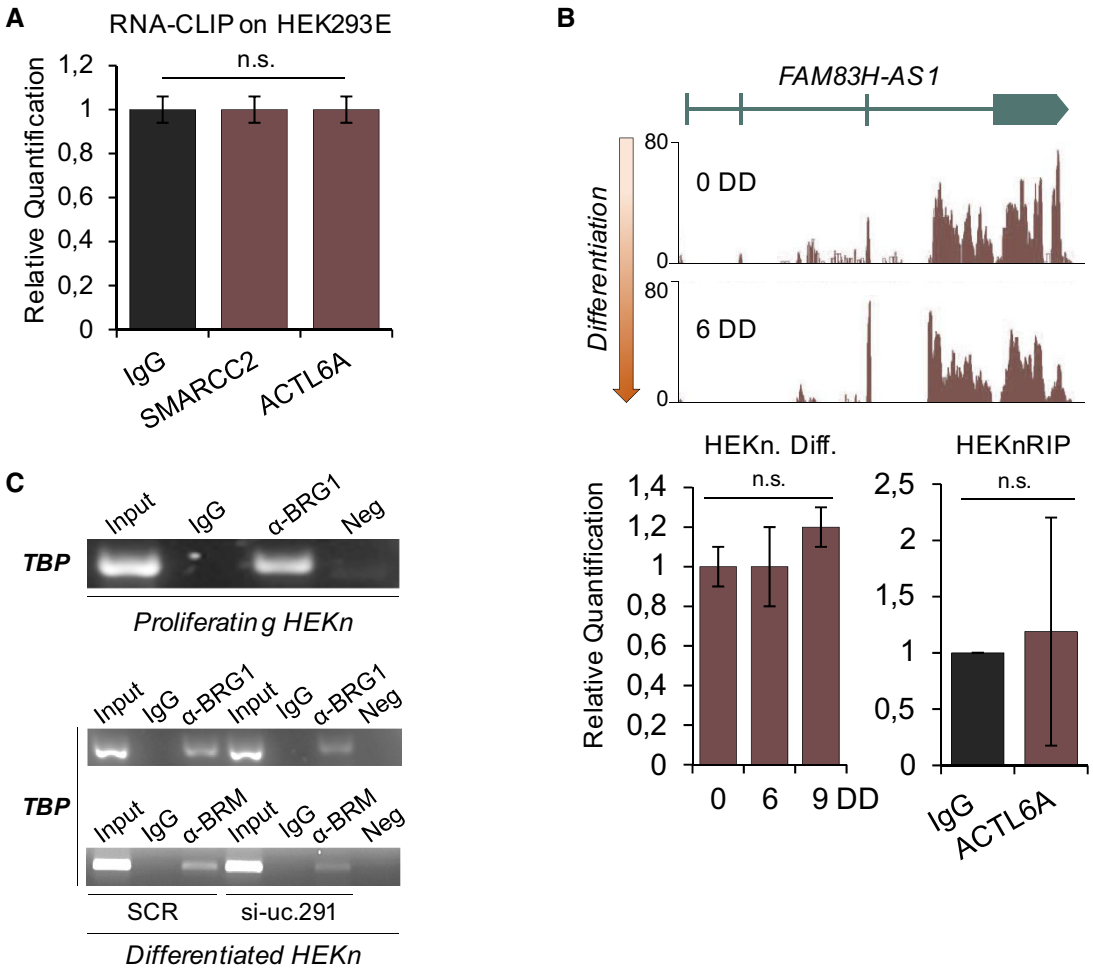

Figure EV5. Negative controls for RIP, CLIP and ChIP.

A RT–qPCR amplifying the lncRNA FAM83H-AS1 used as negative control in the RNA-CLIP experiment (Fig 4C). Note that FAM83H-AS1 resulted expressed in HEK293E (C_t mean in the input = 26.3, data not shown) but was undetectable in all the immunoprecipitated samples (IgG, SMARCC2, ACTL6A). The same samples of Fig 4C were used (n = 3 technical); n.s. = not significant, Student's t-test; HEK293 = human embryonic kidney 293.

B FAM83H-AS1 was used as negative control for the RIP performed in HEKn (Fig 4D). On top, RNA sequencing in HEKn (from Ref. 8) showing FAM83H-AS1 expression is unchanged during keratinocyte differentiation. On bottom, RT–qPCR confirming FAM83H-AS1 is not modulated during the *in vitro* differentiation process (left histogram; same samples of Fig 1B (n = 4 different human donors) were used) and it does not interact with ACTL6A (right histogram; same samples of Fig 4D (n = 3 replicates on 1 human donor) were used); n.s. = not significant, Student's t-test; DD = days of differentiation.

C On the top, end-point PCR of TATA-box-binding protein (TBP) promoter after BRG1 chromatin IP in proliferating HEKn. On the bottom, end-point PCR of TBP promoter after BRG1 (*upper agarose gel*) and BRM (*lower agarose gel*) ChIP in differentiated HEKn silenced for uc.291. The same samples of Fig 5 were used.